
CAUSALITY \neq INVARIANCE: FUNCTION AND CONCEPT VECTORS IN LLMs

000
001
002
003
004
005 **Anonymous authors**
006 Paper under double-blind review
007
008
009
010
011
012
013
014
015
016
017
018
019
020
021
022
023
024
025
026
027
028
029
030
031
032
033
034
035
036
037
038
039
040
041
042
043
044
045
046
047
048
049
050
051
052
053

ABSTRACT

Do large language models (LLMs) represent concepts abstractly, i.e., independent of input format? We revisit Function Vectors ($\mathcal{F}\mathcal{V}$ s), compact representations of in-context learning (ICL) tasks that causally drive task performance. Across multiple LLMs, we show that $\mathcal{F}\mathcal{V}$ s are not fully invariant: $\mathcal{F}\mathcal{V}$ s of the same concept are nearly orthogonal when extracted from different input formats (e.g., open-ended vs. multiple-choice). We introduce Concept Vectors ($\mathcal{C}\mathcal{V}$ s) which produce more stable concept representations. Like $\mathcal{F}\mathcal{V}$ s, $\mathcal{C}\mathcal{V}$ s are composed of attention head outputs; however, unlike $\mathcal{F}\mathcal{V}$ s, head selection is optimized via Representational Similarity Analysis (RSA) to encode concepts consistently across input formats. While these heads emerge in similar layers to $\mathcal{F}\mathcal{V}$ -related heads, the two sets are largely distinct, suggesting different underlying mechanisms. Steering experiments reveal that $\mathcal{F}\mathcal{V}$ s excel in-distribution, when extraction and application formats match (e.g., both open-ended in English), while $\mathcal{C}\mathcal{V}$ s generalize better out-of-distribution across both question types (open-ended vs. multiple-choice) and languages. Our results show that LLMs do contain abstract concept representations, but these differ from those that drive ICL performance.

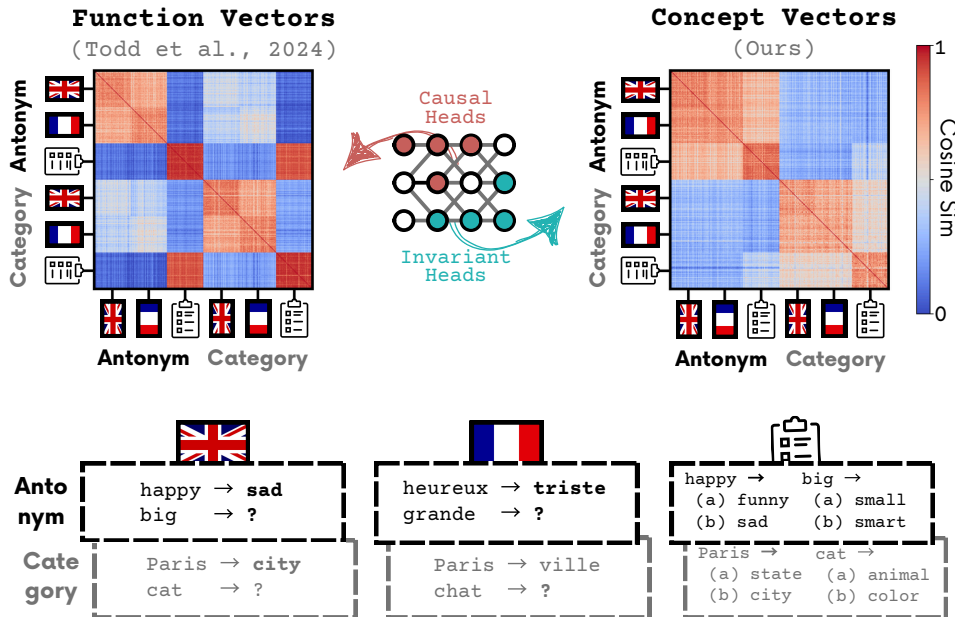


Figure 1: *Function vs. Concept Vectors*. **Top:** Similarity matrices for $\mathcal{F}\mathcal{V}$ s (left) and $\mathcal{C}\mathcal{V}$ s (right) in Llama 3.1 70B; cells show how similar two prompt representations are (warmer = more similar). **Middle:** Schematic highlighting the distinction between heads with causal effect (AP-selected) and heads that encode format-invariant structure (RSA-selected). **Bottom:** Example prompts for two concepts across three formats (EN open-ended, FR open-ended, multiple-choice). **Takeaway:** $\mathcal{F}\mathcal{V}$ s cluster by input format; $\mathcal{C}\mathcal{V}$ s cluster by concept across formats.

054 1 INTRODUCTION
055

056 Do large language models represent concepts abstractly, i.e., in a way that is stable across surface
057 form? We focus on *relational concepts*: mappings between entities, such as linking a word to its
058 antonym. Cognitive science has long argued that abstract representation of such structure underlies
059 human generalization (Gentner, 1983; Hofstadter, 1995; Mitchell, 2020). This capability allows
060 identifying that “hot → cold” and “big → small” share the same oppositional relation, independent of
061 the specific words or how the task is presented. Recent work shows that LLMs exhibit representational
062 structures similar to humans (Pinier et al., 2025; Du et al., 2025; Doerig et al., 2025), raising the
063 question: *do the abstract representations hypothesized to support analogical reasoning actually drive
064 LLM performance on such tasks?*

065 We find that LLMs do contain abstract relational concept information, but the components that encode
066 it differ from those that causally drive in-context learning (ICL) behavior. This separation challenges
067 the *single-circuit hypothesis* that format-invariant representations are what primarily enable ICL.

068 We revisit Function Vectors ($\mathcal{F}\mathcal{V}$ s)—compact vectors formed by summing outputs of a small set of
069 attention heads that mediate ICL (Todd et al., 2024; Hendel et al., 2023; Yin & Steinhardt, 2025).
070 Because $\mathcal{F}\mathcal{V}$ s transfer across contexts (e.g., differently formatted prompts and natural text), they are
071 often treated as encoding the underlying concept (Zheng et al., 2024; Griffiths et al., 2025; Bakalova
072 et al., 2025; Brumley et al., 2024; Fu, 2025). We update this view: $\mathcal{F}\mathcal{V}$ s are not fully invariant. For
073 the same concept, $\mathcal{F}\mathcal{V}$ s extracted from different input formats (open-ended vs. multiple-choice) are
074 nearly orthogonal, indicating that $\mathcal{F}\mathcal{V}$ s mix concept with format (§2.2.1).

075 To isolate format-invariant structure, we contrast *activation patching* (AP), which localizes compo-
076 nents with causal effects on outputs, with *representational similarity analysis* (RSA) (Kriegeskorte,
077 2008), which localizes components whose representations organize by concept independent of for-
078 mat. Using RSA to select heads and then summing their activations yields Concept Vectors ($\mathcal{C}\mathcal{V}$ s).
079 Across seven relational concepts, three input formats (open-ended English, open-ended French,
080 multiple-choice), and four models (Llama 3.1 8B/70B; Qwen 2.5 7B/72B), we find that $\mathcal{C}\mathcal{V}$ heads
081 arise in similar layers but are largely disjoint from $\mathcal{F}\mathcal{V}$ heads, suggesting separable mechanisms for
082 invariance vs. causality (§2.2.2).

083 Finally, we test whether $\mathcal{C}\mathcal{V}$ s can steer. In steering experiments, $\mathcal{F}\mathcal{V}$ s produce larger in-distribution
084 gains when extraction and application formats match (§3.2.1), whereas $\mathcal{C}\mathcal{V}$ s generalize more con-
085 sistently out-of-distribution across question type and language (§3.2.2) and produce fewer format
086 artifacts (e.g., tokens and language from extraction prompts; §3.2.3).

087 Overall, our contributions are as follows:

- **$\mathcal{F}\mathcal{V}$ s are not input-invariant.** They mix relational concepts with input format; same-concept
 $\mathcal{F}\mathcal{V}$ s differ sharply across formats.
- **RSA reveals $\mathcal{C}\mathcal{V}$ heads.** These heads encode relational concepts at a higher level of
abstraction than $\mathcal{F}\mathcal{V}$ heads.¹
- **$\mathcal{C}\mathcal{V}$ and $\mathcal{F}\mathcal{V}$ heads are disjoint.** $\mathcal{F}\mathcal{V}$ s and $\mathcal{C}\mathcal{V}$ s are realized by different attention heads,
suggesting that abstract concept representations are distinct from the mechanisms that
causally drive ICL performance.
- **Steering trade-off.** $\mathcal{F}\mathcal{V}$ s steer more strongly in-distribution, while $\mathcal{C}\mathcal{V}$ s generalize more
consistently out-of-distribution, albeit with smaller absolute gains.

100 2 IN SEARCH OF INVARIANCE
101

103 We test whether concept representations are stable across surface form, using AP (causal heads) and
104 RSA (format-invariant heads) across models, datasets, and formats. We then form Function/Concept
105 Vectors to compare clustering by format vs. concept; AP/RSA heads lie in similar layers but show
106 minimal top-K overlap.

107 ¹We expand on what we mean by “higher level of abstraction” in the Discussion (§5).

108 2.1 METHODS
 109
 110 2.1.1 MODELS
 111
 112 We test Llama 3.1 (8B, 70B) and Qwen 2.5 (7B, 72B) models (Meta AI, 2024; Qwen et al., 2025).
 113 All models are autoregressive, residual-based transformers (Vaswani et al., 2023). Each model, f
 114 internally comprises of \mathcal{L} layers. Each layer is composed of a multi-layer perceptron (MLP) and
 115 J attention heads $a_{\ell j}$ which together produce the vector representation of the last token of layer ℓ ,
 116 $\mathbf{h}_\ell = \mathbf{h}_{\ell-1} + \text{MLP}_\ell + \sum_{j \in J} a_{\ell j}$ (Elhage et al., 2021).

117 2.1.2 TASKS
 118
 119 **Datasets** We define a dataset as one concept expressed in one input format (e.g., Antonym in open-
 120 ended English). For each dataset we build a set of in-context prompts $P_d = \{p_d^i\}$ where i indexes
 121 individual prompts within dataset d . Each prompt contains few-shot input–output examples (x, y)
 122 that illustrate the same concept, followed by a query input x_q^i whose target output y_q^i is withheld. The
 123 input–output pairs (x, y) were either sourced from prior work or generated using OpenAI’s GPT-4o
 124 (see Appendix D for details). Example prompts are provided in Appendix A.

125 **Concepts.** We consider seven concepts:

126 • **Antonym** Map a word to one with opposite meaning (e.g., hot → cold).
 127 • **Categorical** Map a word to its semantic category (e.g., apple → fruit).
 128 • **Causal** Map a cause to an effect (e.g., rain → wet).
 129 • **Synonym** Map a word to one with similar meaning (e.g., big → large).
 130 • **Translation** Translate a word to another language (e.g., house → maison).
 131 • **Present–Past** Convert a verb from present to past tense (e.g., run → ran).
 132 • **Singular–Plural** Convert a noun from singular to plural (e.g., cat → cats).

133 **Input formats.** We vary only the prompt’s surface format; the (x, y) relation stays the same. Formats:

134 • Open-ended ICL in English (OE–EN)
 135 • Open-ended ICL in a different language (French or Spanish; OE–FR or OE–ES)
 136 • Multiple-choice ICL in English (MC)

137 We use 5-shot prompts for open-ended and 3-shot for multiple-choice to reduce computational load
 138 given prompt length. Altogether, we have 21 datasets (7 concepts \times 3 input formats). We build 50
 139 prompts per dataset (total $N = 1050$ prompts).

140 2.1.3 ACTIVATION PATCHING

141 Activation patching replaces specific activations with cached ones from a *clean* run to assess their im-
 142 pact on the model’s output. The cached activations are then inserted into selected model components
 143 in a *corrupted* run, where the systematic relationships in the prompt are disrupted. For example, in
 144 an antonym ICL task, consider a *clean prompt*: Hot → **Cold**, Big → **Small**, Clean → **?** and a *corrupted prompt*: House → Cold, Eagle → Small, Clean → **?** The goal of
 145 activation patching is then to localize model components that push the model to the correct answer,
 146 **Dirty**, on the corrupted prompt.

147 We compute the *causal indirect effect* (CIE) for each attention head $a_{\ell j}$ as the difference between
 148 the probability of predicting the expected token y when processing the corrupted prompt \tilde{p} with and
 149 without the transplanted mean activation $\bar{a}_{\ell j}$ from clean runs:

$$\text{CIE}(a_{\ell j}) = f(\tilde{p} \mid \mathbf{a}_{\ell j} := \bar{a}_{\ell j})[y] - f(\tilde{p})[y] \quad (1)$$

150 We then compute the *average indirect effect* (AIE) over a collection \mathcal{D} of all datasets (§2.1.2). ²

$$\text{AIE}(a_{\ell j}) = \frac{1}{|\mathcal{D}|} \sum_{d \in \mathcal{D}} \frac{1}{|\tilde{\mathcal{P}}_d|} \sum_{\tilde{p}_i \in \tilde{\mathcal{P}}_d} \text{CIE}(a_{\ell j}) \quad (2)$$

151 where $\tilde{\mathcal{P}}_d$ denotes the set of corrupted prompts for dataset d .

152 ²*Note:* Unlike Todd et al. (2024) we compute AIE scores across all input formats, not OE–ENG only.

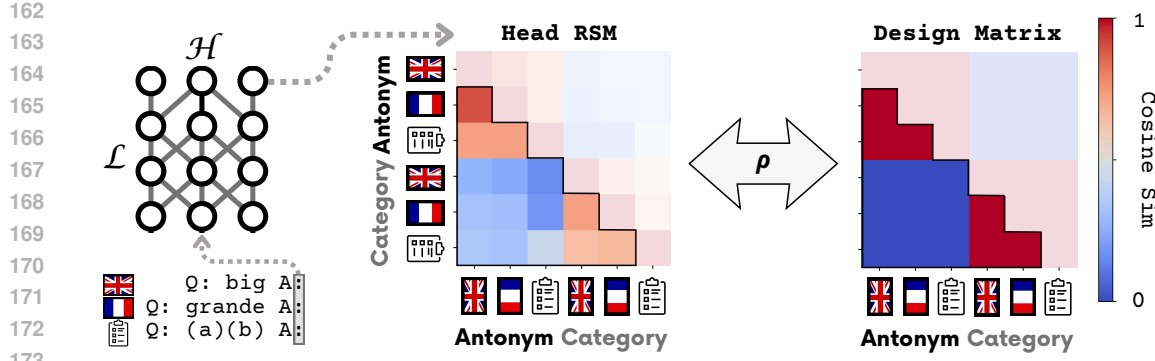


Figure 2: *Representational Similarity Analysis (RSA)*. For each attention head, we compute a representational similarity matrix (RSM) over prompts spanning concepts and input formats (cosine similarity of head outputs). We construct a binary design matrix that marks pairs sharing the same concept, independent of format. The RSA score for a head is Spearman’s ρ between the lower-triangular entries of the RSM and the design matrix; higher ρ indicates stronger concept-invariant encoding.

2.1.4 REPRESENTATIONAL SIMILARITY ANALYSIS

To find attention heads encoding concepts invariant to input formats, we employ representational similarity analysis (RSA; Kriegeskorte (2008)).

For each attention head $a_{\ell j}$ we compute representational similarity matrices (RSMs) where v_i denotes the output extracted from $a_{\ell j}$ for the i th prompt $p_i \in P_N$, and $\theta(\cdot, \cdot)$ is a cosine similarity function.

$$\text{RSM} = \begin{bmatrix} 1 & \dots & \theta(v_1, v_N) \\ \vdots & \ddots & \vdots \\ \theta(v_N, v_1) & \dots & 1 \end{bmatrix} \quad (3)$$

We then construct a binary design matrix, DM, where each entry is set to 1 if the corresponding pair of prompts share the same attribute value, and 0 otherwise. In this paper, we consider two attributes: (1) concept - does a pair of prompts illustrate the same concept, regardless of the input format? and (2) prompt_format - does a pair of prompts have the same question type (i.e. open-ended or multiple-choice)?

We then quantify the alignment between the RSM and DM for the lower-triangles (since similarity matrices are symmetric) using the non-parametric Spearman’s rank correlation coefficient (ρ).

To localize attention heads carrying invariant concept information we compute the RSA for each attention head obtaining a single Concept RSA score for each attention head.

$$\text{Concept-RSA}(a_{\ell j}) = \rho(\text{RSM}_{\ell j}, \text{Concept-DM}) \quad (4)$$

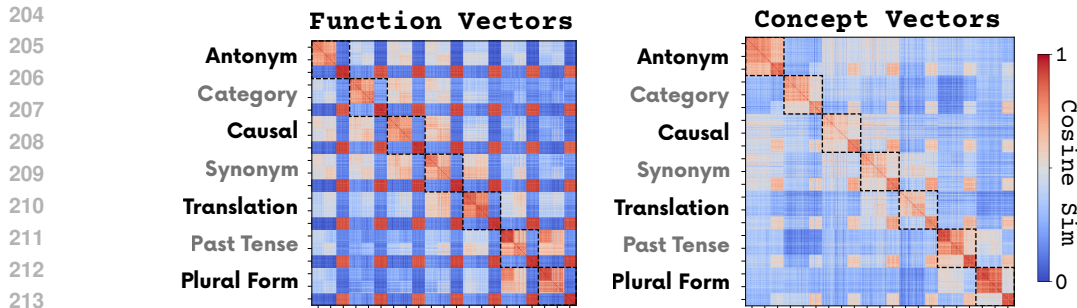
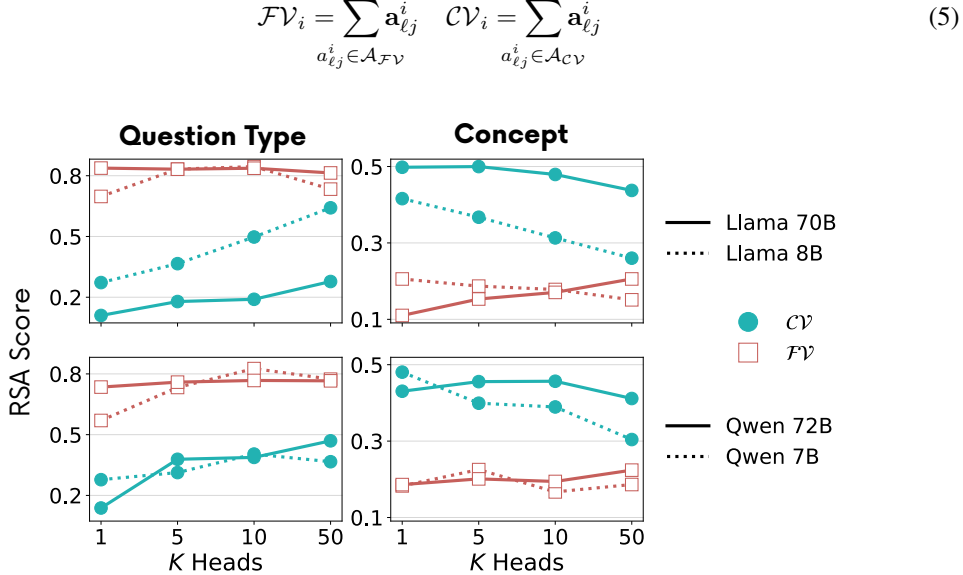


Figure 3: *Similarity matrices*. Full similarity matrices extracted from top $K = 5$ heads in \mathcal{CV} s and \mathcal{FV} s in Llama 3.1 70B for all concepts. See Appendix B for other models.

216 2.1.5 FUNCTION & CONCEPT VECTORS
217

218 To form Function/Concept Vectors we create sets of top K ranking attention heads, $\mathcal{A}_{\mathcal{F}\mathcal{V}}$ and $\mathcal{A}_{\mathcal{C}\mathcal{V}}$,
219 based on their AIE and RSA scores respectively. Function/Concept Vectors for prompt i are then
220 computed as the sum of activations for this prompt, $\mathbf{a}_{\ell j}^i$, from the sets $\mathcal{A}_{\mathcal{F}\mathcal{V}}$ and $\mathcal{A}_{\mathcal{C}\mathcal{V}}$ respectively.



2.2 RESULTS

2.2.1 CONCEPT VECTORS ARE MORE INVARIANT TO INPUT FORMAT

248 We test invariance to input format by computing RSA with design matrices for concept and question
249 type (following the setup in §2.1.4). We form $\mathcal{F}\mathcal{V}$ s/ \mathcal{CV} s by summing the top- K heads ranked by
250 AIE/RSA (Eq. 5). Across models and K , \mathcal{CV} s show higher concept RSA and lower question-type
251 RSA than $\mathcal{F}\mathcal{V}$ s (Figure 4), indicating that $\mathcal{F}\mathcal{V}$ s encode format more strongly while \mathcal{CV} s track concept.
252 Consistently, similarity matrices for Llama 3.1 70B cluster by concept across formats for \mathcal{CV} s, but
253 by format for $\mathcal{F}\mathcal{V}$ s (Figure 3), where within-format type $\mathcal{F}\mathcal{V}$ clusters are nearly identical with mean
254 cosine similarity = 0.90. \mathcal{CV} s nonetheless exhibit a weaker within-format type cluster (mean cosine
255 similarity = 0.55), suggesting they retain some low-level format information. Overall, however, \mathcal{CV} s
256 remain markedly more invariant to input format than $\mathcal{F}\mathcal{V}$ s.

Model	K=3	K=5	K=10	K=20	K=50	K=100
Llama-3.1 8B	0	0	1	1	12	28
Llama-3.1 70B	0	0	0	0	1	6
Qwen2.5 7B	0	0	0	4	15	39
Qwen2.5 72B	0	0	0	1	3	13

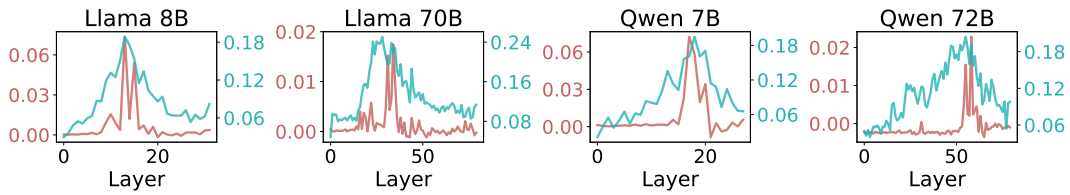
262
263 Table 1: *RSA–AIE head overlap*. Overlap between RSA and AIE heads (number of overlapping
264 heads among top- K). Bold numbers indicate overlap significantly above chance ($p < 0.05$; details in
265 Appendix E). **Takeaway:** $\mathcal{F}\mathcal{V}$ s and \mathcal{CV} s are composed of different attention heads.

2.2.2 FUNCTION & CONCEPT VECTORS ARE COMPOSED OF DIFFERENT ATTENTION HEADS

266 If we compare which heads are selected by the two procedures, we see that $\mathcal{F}\mathcal{V}$ s and \mathcal{CV} s are
267 composed of different attention heads. First, we ranked each head for each method, i.e., AIE (§2.1.3)

270 for $\mathcal{F}\mathcal{V}$ s and by Concept-RSA (§2.1.4) for $\mathcal{C}\mathcal{V}$ s. Then we examined depth and top- K overlap. Layer-
271 averaged scores show similar layer profiles (Figure 5), but head identities barely overlap: for $K \leq 20$
272 the intersection is near zero and stays small at larger K (Table 1). We also note that AIE scores are
273 highly sparse: their histogram peaks at zero with a long right tail (Figure 12)—so only a few heads
274 have measurable causal effect. Together this supports that AIE-selected *causal* heads are largely
275 distinct from the *invariant*, RSA-selected heads.

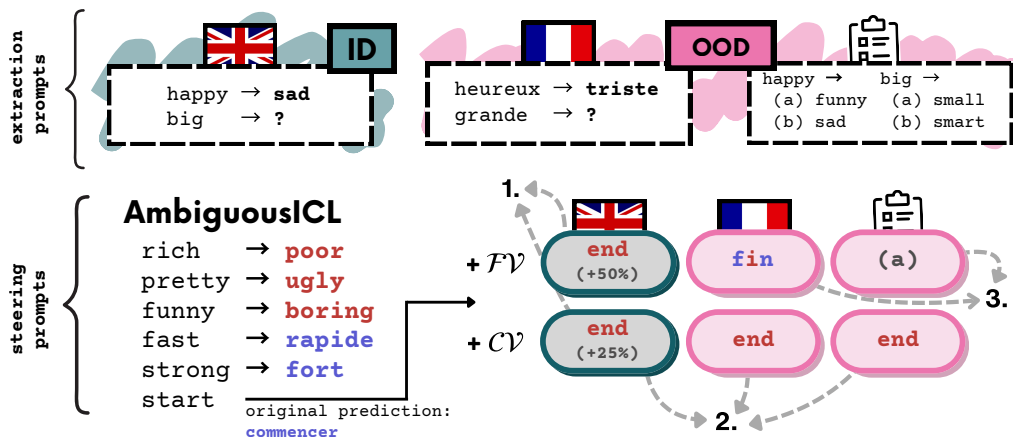
276 To ensure this separation is not an artifact of patching within the same format, we also performed
277 cross-format activation patching (e.g., extracting activations from open-ended prompts and patching
278 them into multiple-choice). This procedure continued to identify the same FV heads and did not
279 identify CV heads (see Appendix O), confirming that FVs are the primary causal drivers regardless
280 of input format.



291 Figure 5: *Layer-wise AIE vs. RSA*. AIE and RSA scores averaged across all heads per layer.
292 **Takeaway:** $\mathcal{F}\mathcal{V}$ and $\mathcal{C}\mathcal{V}$ heads are in similar layers.

293 3 CAN CONCEPT VECTORS STEER?

294 We now test whether these invariant heads can steer: we introduce how we construct vectors, the
295 AmbiguousICL setup with conflicting cues, and the intervention protocol. $\mathcal{F}\mathcal{V}$ s win in-distribution;
296 $\mathcal{C}\mathcal{V}$ s transfer better out-of-distribution with fewer format artifacts, at a cost of smaller gains.



313 Figure 6: *Overview of steering results*. **Top:** We extract $\mathcal{C}\mathcal{V}$ s and $\mathcal{F}\mathcal{V}$ s from antonym ICL prompts
314 in formats that are in-distribution (ID; OE-ENG) or out-of-distribution (OOD; OE-FR, MC) relative
315 to the AmbiguousICL task (bottom-left). **Bottom-left:** We interleave two concepts—**antonym** and
316 **EN→FR translation**—within one prompt; the model’s original prediction is the French translation.
317 **Bottom-right:** Predictions after steering. **Takeaways:** (1) $\mathcal{F}\mathcal{V}$ s yield larger ID gains. (2) $\mathcal{C}\mathcal{V}$ s show
318 more stable OOD effects across formats. (3) $\mathcal{F}\mathcal{V}$ s can conflate concept with input format (e.g., French
319 version of antonym and multiple-choice formatting).

320 3.1 STEERING METHODS

321 **Steering Vectors Construction.** For each concept and input format (OE-ENG, OE-FR, MC), we
322 compute for every selected head $a_{\ell j}$ the mean last-token activation across the 50 *extraction prompts*

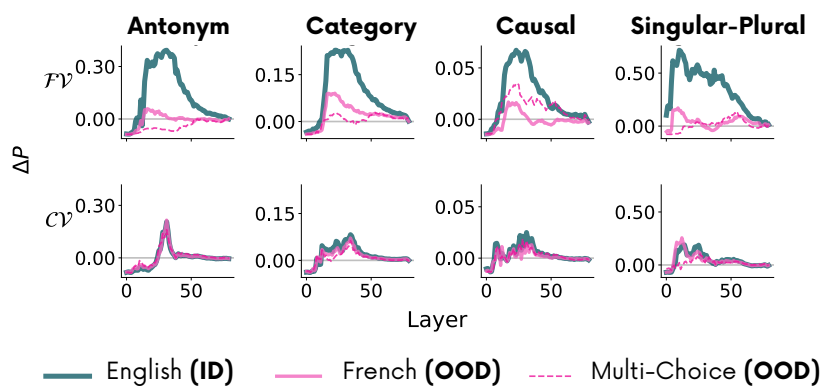
324 of that concept–format. We then form one vector per format by summing these mean activations
 325 over the top- K heads selected for \mathcal{CV} or \mathcal{FV} (as in Eq. 5, but using per-format means in place of
 326 per-prompt activations). This yields one ID vector (OE–ENG) and two OOD vectors (OE–FR, MC)
 327 per concept.

328 **AmbiguousICL Task.** We evaluate on AmbiguousICL tasks (Figure 6): each prompt interleaves two
 329 concepts (3 then 2 exemplars) followed by a query. The second concept is always English→French
 330 translation. Unsteered models tend to continue with the second concept; we aim to steer toward
 331 the first. Note that steering prompts are distinct from the extraction prompts used to construct the
 332 vectors. This setup is diagnostic: it tests whether representations encode abstract relational structure
 333 independent of extraction prompts’ surface format. To perform well in this setup requires consistency
 334 between ID and OOD performance.

335 **Steering with \mathcal{CV} s and \mathcal{FV} s.** We add a vector \mathbf{v} to the last-token residual stream at a chosen layer:

$$\mathbf{h}_\ell \leftarrow \mathbf{h}_\ell + \alpha \mathbf{v} \quad (6)$$

336 We measure effectiveness as $\Delta P = P_{\text{after}}(y) - P_{\text{before}}(y)$, averaged over 100 prompts per concept
 337 (see Figure 22 for Top-1 accuracy). We sweep α and K and report the best per model (Appendix F).



354 Figure 7: *Steering effect across layers.* We inject \mathcal{CV} s and \mathcal{FV} s into Llama-3.1-70B and plot the
 355 change in target-token probability (ΔP) for four representative concepts (columns). Curves compare
 356 ID extraction format with OOD formats relative to the AmbiguousICL task (Figure 6). Higher
 357 ΔP means the model assigns more probability to the expected token than the unsteered model.
 358 **Takeaways:** (1) \mathcal{FV} s typically achieve larger ID gains but often drop OOD. (2) \mathcal{CV} s yield smaller
 359 gains yet show more stable OOD behavior across formats. See Figure 16 for other concepts/models.

3.2 STEERING RESULTS

3.2.1 FUNCTION VECTORS OUTPERFORM CONCEPT VECTORS IN DISTRIBUTION

365 Extracted from OE–ENG (ID setting), \mathcal{FV} s yield the largest gains on ambiguous prompts (Figure 7).
 366 \mathcal{CV} s also help but with smaller ΔP and minimal zeroshot effect (Figure 17). At the token level both
 367 vectors lift plausible English antonyms in the ID case (Table 2).

3.2.2 CONCEPT VECTORS ARE MORE STABLE OUT OF DISTRIBUTION

371 **Performance gains (ΔP).** Out of distribution (extracting vectors from OE–FR or MC), \mathcal{CV} s more
 372 often maintain positive effects across formats, whereas \mathcal{FV} s frequently degrade—especially for
 373 MC—and only occasionally stay consistent for specific concepts/models (Figs. 7, 16). \mathcal{CV} s raise the
 374 probability of the correct English answer across formats, and their top- Δ tokens remain concept-
 375 aligned (Table 2). Crucially, the key finding is not absolute performance but consistency: \mathcal{CV} s
 376 increase the probability of producing similar concept-aligned tokens regardless of extraction format.

377 **Distributional consistency (KL).** To quantify consistency across formats independent of absolute
 378 gains, we compare the model’s next-token distributions after steering with ID and OOD vectors. For

378 **Query:** salty →

	+ Antonym	Top Δ Tokens
$\mathcal{F}\mathcal{V}$	OE-ENG	<u>sweet</u> (+56%), <u>fresh</u> (+16%), <u>bland</u> (+6%), <u>taste</u> (+3%), <u>uns</u> (+2%)
	OE-FR	<u>su</u> (+31%), <u>dou</u> (+27%), <u>frais</u> (+5%), <u>fade</u> (+5%), <u>ins</u> (+3%)
	MC	<u>(</u> (+53%), <u>A</u> (+1%), <u>\n</u> (+1%), <u>space</u> (+0%), <u>)</u> (+0%)
$\mathcal{C}\mathcal{V}$	OE-ENG	<u>sweet</u> (+49%), <u>fresh</u> (+8%), <u>bland</u> (+3%), <u>taste</u> (+3%), <u>uns</u> (+3%)
	OE-FR	<u>sweet</u> (+54%), <u>fresh</u> (+9%), <u>bland</u> (+3%), <u>uns</u> (+3%), <u>taste</u> (+2%)
	MC	<u>sweet</u> (+35%), <u>fresh</u> (+12%), <u>bland</u> (+4%), <u>uns</u> (+3%), <u>taste</u> (+3%)

387 Table 2: *Token-level steering effects*. Top tokens with largest probability gains when injecting $\mathcal{C}\mathcal{V}$ s or
388 $\mathcal{F}\mathcal{V}$ s into Llama-3.1-70B on the AmbiguousICL prompt (query shown above). Results shown at the
389 layer with the strongest in-distribution effect per vector. Without intervention, the model predicts
390 French sa (from *sale*) with 49%; antonym sweet has 2%. English antonyms in red, French in
391 blue, and the opening bracket (MC token) in green.

392
393

394 each concept and vector type, we select the top 5 layers that achieve the highest ID ΔP . At each
395 selected layer we compute KL divergence

$$D_{KL} [p(\mathbf{x} | \mathbf{v}_{OOD}) \| p(\mathbf{x} | \mathbf{v}_{ID})]$$

399 between the post-intervention distributions at the query token, where lower values indicate more
400 similar effects of ID and OOD vectors. We average this KL divergence over prompts and selected
401 layers to obtain one score per concept, and then summarize per model (Figure 8). Across models,
402 $\mathcal{C}\mathcal{V}$ s yield lower KL than $\mathcal{F}\mathcal{V}$ s. The CV–FV KL gap is larger for MC than for OE–FR.

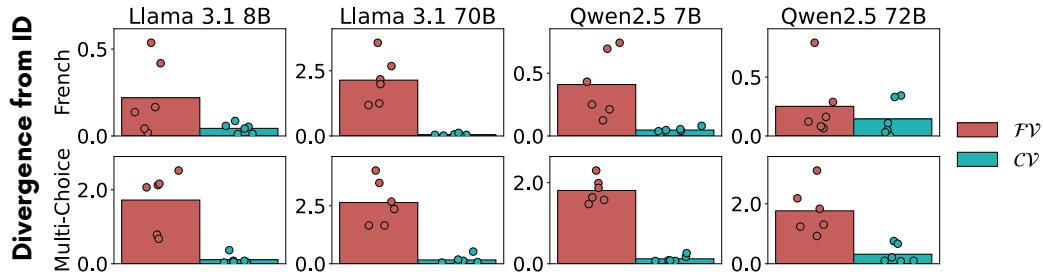
403

404 3.2.3 FUNCTION VECTORS MIX CONCEPT WITH INPUT FORMAT

405

406 Out of distribution, $\mathcal{F}\mathcal{V}$ s reflect both prompt format and concept. When vectors are extracted from
407 OE–FR, they push the model toward the French translation of the concept (e.g., French antonyms),
408 and when extracted from MC, they increase the probability of format tokens such as the opening
409 bracket (Table 2). We quantify the language effect by measuring ΔP for the French translation
410 across concepts (Figure 13). In the larger models, $\mathcal{F}\mathcal{V}$ s substantially increase the probability of the
411 French token, whereas $\mathcal{C}\mathcal{V}$ s remain near zero; in smaller models the effect is negligible. Notably, $\mathcal{F}\mathcal{V}$ s
412 extracted from open-ended Spanish prompts induce almost the same bias toward the French translation
413 as $\mathcal{F}\mathcal{V}$ s extracted from French prompts (Figure 14), even though the AmbiguousICL alternatives are
414 French only. This pattern suggests that $\mathcal{F}\mathcal{V}$ s capture a generic translation/foreign-language signal
415 tied to the extraction format rather than language-specific content. Combined with the MC bracket
416 effect (Figure 15), these findings indicate that $\mathcal{F}\mathcal{V}$ s mix concept with surface format, while $\mathcal{C}\mathcal{V}$ s are
417 comparatively format-invariant.

418



419 Figure 8: *Consistency of steering effects*. KL divergence between the probability distributions after
420 the models were steered with an ID (OE-ENG) and OOD vectors (OE-FR [top], MC [bottom]).
421 Lower values indicate more similar effects of ID and OOD vectors. **Takeaway:** $\mathcal{C}\mathcal{V}$ s steer the models
422 more consistently than $\mathcal{F}\mathcal{V}$ s.

432 4 RELATED WORK 433

434 **Attention Head Categorization.** Recent work has made significant progress in characterizing
435 specialized attention heads that process in-context learning (ICL) tasks. For instance, Olsson et al.
436 (2022) identified induction-heads, which Yin & Steinhardt (2025) found can develop into \mathcal{FV} -heads
437 during training. Other specialized head types include semantic-induction heads (Ren et al., 2024),
438 symbol-abstraction heads (Yang et al., 2025), and various others (Zheng et al., 2024). Our work
439 extends this line of research by identifying \mathcal{CV} heads, attention heads that invariantly represent
440 concepts in ICL tasks at high levels of abstraction.

441 **Linear Representation of Concepts.** A substantial body of research has established that concepts
442 are represented linearly in LLMs’ representational space (Mikolov et al., 2013; Arora et al., 2016;
443 Elhage et al., 2022). This phenomenon, often termed the “Linear Representation Hypothesis” (Park
444 et al., 2024), has been extensively studied across various tasks and domains. Hernandez et al. (2024)
445 demonstrated that relational concepts—similar to those we study in this paper—can be decoded from
446 LLM activations using linear approximation. Subsequent work by Merullo et al. (2025) revealed
447 that the success of such decoding depends on the frequency of concepts in the pretraining corpora,
448 which may explain why some concepts are represented more consistently than others in our study.
449 Our findings contribute to this literature in two ways: (1) providing further support for the Linear
450 Representation Hypothesis, and (2) extending previous work on relational concept representations by
451 localizing specific attention heads that carry such representations and demonstrating their invariance
452 to input formats.

453 **Symbolic-like reasoning in LLMs.** Recent work has demonstrated that LLMs can exhibit symbol-
454 like representational properties even without explicit symbolic architecture (Feng & Steinhardt, 2024;
455 Yang et al., 2025; Griffiths et al., 2025). Yang et al. (2025) define symbolic processing as requiring
456 two key properties: (1) invariance to content variations, and (2) indirection through pointers rather
457 than direct content storage. Our \mathcal{CV} s exhibit both properties: they are invariant to input format
458 changes and function as pointers to content stored elsewhere, unlike \mathcal{FV} s which directly store content
459 (§3.2.3).

460 5 DISCUSSION 461

462 Our results separate two representational roles in LLMs: components that *cause* strong ICL perfor-
463 mance and components that *encode* abstract concept structure. Function Vectors (\mathcal{FV} s) occupy the
464 first role, steering models effectively when extraction and application formats match, but deteriorating
465 out of distribution (formats/languages). Conversely, Concept Vectors (\mathcal{CV} s) built from RSA-selected
466 heads encode concepts at a *higher level of abstraction* and generalize more robustly across languages
467 and question types, albeit with smaller causal effects. This supports a view that invariance and
468 causality are mediated by largely distinct mechanisms in similar layers.

469 **Layers of abstraction.** We define abstraction as encoding relational structure (e.g., “antonym”)
470 while discarding surface details (e.g., “English, multiple-choice”). Our results suggest \mathcal{FV} s do
471 capture abstract task information: they reliably encode concepts within a format (Figure 19) and are
472 causally effective even across formats (Appendix O). However, their orthogonality across formats
473 and retention of surface signals (e.g., MC brackets) reveal that they conflate this abstract content with
474 surface form. In contrast, \mathcal{CV} s cluster by concept regardless of format. Thus, \mathcal{FV} s operate at a lower
475 level of abstraction (“antonym in MC format”), while \mathcal{CV} s operate at a higher level (“antonym”),
476 independent of surface form.

477 **Relation to Function Vectors.** Prior work shows that \mathcal{FV} s compactly mediate ICL and can transfer
478 across contexts (Todd et al., 2024). We refine this: \mathcal{FV} portability is strong within families of prompts,
479 but is not fully invariant to surface format. Same-concept \mathcal{FV} s extracted from different formats are
480 nearly orthogonal and can carry language/format signals (e.g., French subword or multiple-choice
481 bracket tokens), while \mathcal{CV} s track concept across formats with less surface content. This distinction
482 can be framed as *equivariance* vs. *invariance*: \mathcal{FV} s adapt to extraction format (e.g., producing
483 French antonyms from French prompts, MC formatting tokens from MC prompts), whereas \mathcal{CV} s
484 steer toward similar outputs regardless of format. Finally, we do not propose \mathcal{CV} s as competitors
485 to \mathcal{FV} s, but rather highlight a mechanistic dissociation: \mathcal{FV} s drive behavior (causality) while \mathcal{CV} s
represent abstract structure (invariance).

486 These findings have implications for theoretical models of ICL, such as recent work by Bu et al.
487 (2025) which posits the retrieval of a single function vector a^f for a function f . Our results suggest
488 this model is incomplete: given the orthogonality of $\mathcal{F}\mathcal{V}$ s across formats, the function vector is better
489 conceptualized as format-conditional $a(f, \phi)$, implying convergence to multiple format-specific
490 basins rather than a single global minimum. Furthermore, we find that $\mathcal{F}\mathcal{V}$ s and $\mathcal{C}\mathcal{V}$ s are orthogonal
491 (even within the same format) which suggests that task representations partition into distinct abstract
492 and format-specific subspaces, rather than residing in a single unified space.

493 **Implications for steering and interpretability.** The dissociation between $\mathcal{F}\mathcal{V}$ s and $\mathcal{C}\mathcal{V}$ s sug-
494 gests a practical trade-off. For *maximal in-distribution control*, $\mathcal{F}\mathcal{V}$ s are preferable. For *robust*
495 *out-of-distribution control* or probing abstract knowledge, $\mathcal{C}\mathcal{V}$ s are more reliable.

496 However, $\mathcal{C}\mathcal{V}$ s appear to require the concept to be already present in the prompt to exert influence. In
497 zero-shot steering (Figure 17) and activation patching—which require inducing or restoring a task
498 "from scratch"— $\mathcal{C}\mathcal{V}$ s are ineffective. In contrast, in AmbiguousICL, where the concept is present
499 but competing, $\mathcal{C}\mathcal{V}$ s successfully steer by amplifying the existing abstract signal. Thus, $\mathcal{F}\mathcal{V}$ s seem
500 necessary to *stantiate* a task, while $\mathcal{C}\mathcal{V}$ s can *modulate* it once present.

501 Methodologically, AP identifies what causally drives behavior, while RSA reveals how representations
502 organize by concept. This distinction highlights that behavioral control and abstract representation
503 can be mediated by different mechanisms.

504 **Analogy and abstract representation.** Hill et al. (2019) propose that "analogies are something like
505 the functions of the mind": concepts achieve their flexibility by being represented abstractly enough
506 to permit context-dependent adaptation across diverse domains of application. This view predicts
507 that relational concepts like *antonym* or *causation* should function identically whether presented
508 as open-ended prompts, multiple-choice questions, or in different languages. Our findings offer a
509 mechanistic refinement: while LLMs do form abstract relational representations ($\mathcal{C}\mathcal{V}$ s), these are
510 largely distinct from the components that causally drive ICL behavior ($\mathcal{F}\mathcal{V}$ s). This dissociation
511 suggests that analogical task performance may not require—or primarily rely on—the most abstract
512 conceptual representations. Instead, LLMs appear to solve ICL tasks via more format-specific
513 mechanisms, even though they do form abstract representations.

514 **Limitations and Future Directions.** Our $\mathcal{C}\mathcal{V}$ head selection targeted heads that encode *all* concepts
515 simultaneously; this global criterion may miss concept-specific heads, which a per-concept RSA
516 could reveal. We also did not probe how $\mathcal{F}\mathcal{V}$ s and $\mathcal{C}\mathcal{V}$ s emerge during model training or how they
517 interact during inference.

518 We propose two possible hypotheses that could be explored in future work:

519 **1. CVs and FVs interact during inference as detection/execution mechanisms.** Previous work by
520 Lindsey et al. (2025) has discovered model features that seem to fire just before the model produces
521 a certain type of output (e.g., a "capital" feature that fires just before the model outputs a name of
522 a capital), and ones that fire more generally when the text mentions different capitals. Other work
523 found that ICL tasks can be understood from an "encoder/decoder" perspective (Han et al., 2025),
524 where the encoder encodes the task into a latent space and the decoder decodes the latent space into
525 the output. Both of these findings suggest that models separate the task encoding and execution into
526 distinct mechanisms which can be linked to $\mathcal{C}\mathcal{V}$ s (encoding/detection) and $\mathcal{F}\mathcal{V}$ s (execution).

527 **2. CVs and FVs do not interact during inference; CVs are simply a backup circuit.** Another
528 possibility is that the two mechanisms are independent. Other works have found *backup circuits*
529 where models can form multiple, partially redundant circuits and compensatory self-repair under
530 ablations (McGrath et al., 2023; Wang et al., 2022). Given that a) both sets of heads are in similar
531 layers (Figure 5), suggesting $\mathcal{C}\mathcal{V}$ s and $\mathcal{F}\mathcal{V}$ s may operate in parallel or via lateral information flow
532 within the residual stream, rather than strict deep-hierarchical dependencies and b) that $\mathcal{C}\mathcal{V}$ heads
533 do not seem to have causal effects in usual ICL tasks (since they were not identified by AP), this
534 hypothesis is also plausible. What is more Davidson et al. (2025) found that different prompting
535 methods yield a different causal tasks representations, therefore it is possible that ICL in LLMs
536 consist of multiple, separate mechanisms.

537
538
539

540 REFERENCES
541

542 Sanjeev Arora, Yuanzhi Li, Yingyu Liang, Tengyu Ma, and Andrej Risteski. A latent variable model
543 approach to PMI-based word embeddings. *Transactions of the Association for Computational
544 Linguistics*, 4:385–399, 2016. doi: 10.1162/tacl_a_00106. URL <https://aclanthology.org/Q16-1028/>.

545

546 Aleksandra Bakalova, Yana Veitsman, Xinting Huang, and Michael Hahn. Contextualize-then-
547 aggregate: Circuits for in-context learning in gemma-2 2b, 2025. URL <https://arxiv.org/abs/2504.00132>.

548

549 Madeline Brumley, Joe Kwon, David Krueger, Dmitrii Krasheninnikov, and Usman Anwar. Com-
550 paring bottom-up and top-down steering approaches on in-context learning tasks, 2024. URL
551 <https://arxiv.org/abs/2411.07213>.

552

553 Dake Bu, Wei Huang, Andi Han, Atsushi Nitanda, Qingfu Zhang, Hau-San Wong, and Taiji Suzuki.
554 Provable in-context vector arithmetic via retrieving task concepts, 2025. URL <https://arxiv.org/abs/2508.09820>.

555

556 Guy Davidson, Todd M. Gureckis, Brenden M. Lake, and Adina Williams. Do different prompting
557 methods yield a common task representation in language models?, 2025. URL <https://arxiv.org/abs/2505.12075>.

558

559 DeepL SE. DeepL translator, 2025. URL <https://www.deepl.com/translator>. Accessed:
560 2025.

561

562 Adrien Doerig, Tim Kietzmann, Emily Allen, Yihan Wu, Thomas Naselaris, Kendrick Kay, and Ian
563 Charest. High-level visual representations in the human brain are aligned with large language
564 models. *Nature Machine Intelligence*, 7:1220–1234, 08 2025. doi: 10.1038/s42256-025-01072-0.

565

566 Changde Du, Kaicheng Fu, Bincheng Wen, Yi Sun, Jie Peng, Wei Wei, Ying Gao, Shengpei Wang,
567 Chuncheng Zhang, Jinpeng Li, Shuang Qiu, Le Chang, and Huiguang He. Human-like object
568 concept representations emerge naturally in multimodal large language models. *Nature Machine
569 Intelligence*, 7(6):860–875, June 2025. ISSN 2522-5839. doi: 10.1038/s42256-025-01049-z. URL
570 <http://dx.doi.org/10.1038/s42256-025-01049-z>.

571

572 Nelson Elhage, Neel Nanda, Catherine Olsson, Tom Henighan, Nicholas Joseph, Ben Mann, Amanda
573 Askell, Yuntao Bai, Anna Chen, Tom Conerly, Nova DasSarma, Dawn Drain, Deep Ganguli, Zac
574 Hatfield-Dodds, Danny Hernandez, Andy Jones, Jackson Kernion, Liane Lovitt, Kamal Ndousse,
575 Dario Amodei, Tom Brown, Jack Clark, Jared Kaplan, Sam McCandlish, and Chris Olah. A
576 mathematical framework for transformer circuits. *Transformer Circuits Thread*, 2021.

577

578 Nelson Elhage, Tristan Hume, Catherine Olsson, Nicholas Schiefer, Tom Henighan, Shauna Kravec,
579 Zac Hatfield-Dodds, Robert Lasenby, Dawn Drain, Carol Chen, Roger Grosse, Sam McCandlish,
580 Jared Kaplan, Dario Amodei, Martin Wattenberg, and Christopher Olah. Toy models of
581 superposition, 2022. URL <https://arxiv.org/abs/2209.10652>.

582

583 Jiahai Feng and Jacob Steinhardt. How do language models bind entities in context?, 2024. URL
584 <https://arxiv.org/abs/2310.17191>.

585

586 Shuhao Fu. *Function Vectors for Relational Reasoning in Multimodal Large Language Models*. PhD
587 thesis, UCLA, 2025.

588

589 Dedre Gentner. Structure-mapping: A theoretical framework for analogy. *Cognitive science*, 7(2):
590 155–170, 1983.

591

592 Thomas L. Griffiths, Brenden M. Lake, R. Thomas McCoy, Ellie Pavlick, and Taylor W. Webb.
593 Whither symbols in the era of advanced neural networks?, 2025. URL <https://arxiv.org/abs/2508.05776>.

594

595 Seungwook Han, Jinyeop Song, Jeff Gore, and Pulkit Agrawal. Emergence and effectiveness
596 of task vectors in in-context learning: An encoder decoder perspective, 2025. URL <https://arxiv.org/abs/2412.12276>.

594 Roee Hendel, Mor Geva, and Amir Globerson. In-Context Learning Creates Task Vectors, October
595 2023.

596

597 Evan Hernandez, Arnab Sen Sharma, Tal Haklay, Kevin Meng, Martin Wattenberg, Jacob Andreas,
598 Yonatan Belinkov, and David Bau. Linearity of relation decoding in transformer language models,
599 2024. URL <https://arxiv.org/abs/2308.09124>.

600

601 Felix Hill, Adam Santoro, David G. T. Barrett, Ari S. Morcos, and Timothy Lillicrap. Learning to
602 make analogies by contrasting abstract relational structure, 2019. URL <https://arxiv.org/abs/1902.00120>.

603

604 Douglas R Hofstadter. *Fluid concepts and creative analogies: Computer models of the fundamental*
605 *mechanisms of thought*. Basic books, 1995.

606

607 Nikolaus Kriegeskorte. Representational similarity analysis – connecting the branches of systems
608 neuroscience. *Frontiers in Systems Neuroscience*, 2008. ISSN 16625137. doi: 10.3389/neuro.06.
609 004.2008.

610

611 Jack Lindsey, Wes Gurnee, Emmanuel Ameisen, Brian Chen, Adam Pearce, Nicholas L. Turner,
612 Craig Citro, David Abrahams, Shan Carter, Basil Hosmer, Jonathan Marcus, Michael Sklar, Adly
613 Templeton, Trenton Bricken, Callum McDougall, Hoagy Cunningham, Thomas Henighan, Adam
614 Jermyn, Andy Jones, Andrew Persic, Zhenyi Qi, T. Ben Thompson, Sam Zimmerman, Kelley
615 Rivoire, Thomas Conerly, Chris Olah, and Joshua Batson. On the biology of a large language
616 model. *Transformer Circuits Thread*, 2025. URL <https://transformer-circuits.pub/2025/attribution-graphs/biology.html>.

617

618 Thomas McGrath, Matthew Rahtz, Janos Kramar, Vladimir Mikulik, and Shane Legg. The hydra
619 effect: Emergent self-repair in language model computations, 2023. URL <https://arxiv.org/abs/2307.15771>.

620

621 Jack Merullo, Noah A. Smith, Sarah Wiegreffe, and Yanai Elazar. On linear representations and
622 pretraining data frequency in language models, 2025. URL <https://arxiv.org/abs/2504.12459>.

623

624

625 Meta AI. The Llama 3 Herd of Models, November 2024.

626

627 Tomas Mikolov, Wen-tau Yih, and Geoffrey Zweig. Linguistic regularities in continuous space word
628 representations. In Lucy Vanderwende, Hal Daumé III, and Katrin Kirchhoff (eds.), *Proceedings*
629 *of the 2013 Conference of the North American Chapter of the Association for Computational Lin-*
630 *guistics: Human Language Technologies*, pp. 746–751, Atlanta, Georgia, June 2013. Association
631 for Computational Linguistics. URL <https://aclanthology.org/N13-1090/>.

632

633 Melanie Mitchell. *Artificial Intelligence: A Guide for Thinking Humans*. Picador, New York, first
634 picador paperback edition, 2020 edition, 2020. ISBN 978-1-250-75804-0.

635

636 Catherine Olsson, Nelson Elhage, Neel Nanda, Nicholas Joseph, Nova DasSarma, Tom Henighan,
637 Ben Mann, Amanda Askell, Yuntao Bai, Anna Chen, Tom Conerly, Dawn Drain, Deep Ganguli,
638 Zac Hatfield-Dodds, Danny Hernandez, Scott Johnston, Andy Jones, Jackson Kernion, Liane
639 Lovitt, Kamal Ndousse, Dario Amodei, Tom Brown, Jack Clark, Jared Kaplan, Sam McCandlish,
640 and Chris Olah. In-context learning and induction heads, 2022. URL <https://arxiv.org/abs/2209.11895>.

641

642 OpenAI. Gpt-4o system card, 2024. URL <https://arxiv.org/abs/2410.21276>.

643

644 Kiho Park, Yo Joong Choe, and Victor Veitch. The Linear Representation Hypothesis and the
645 Geometry of Large Language Models, July 2024.

646

647 Christopher Pinier, Sonia Acuña Vargas, Mariia Steeghs-Turchina, Dora Matzke, Claire E. Stevenson,
648 and Michael D. Nunez. Large language models show signs of alignment with human neurocogni-
649 tion during abstract reasoning, 2025. URL <https://arxiv.org/abs/2508.10057>.

648 Qwen, :, An Yang, Baosong Yang, Beichen Zhang, Binyuan Hui, Bo Zheng, Bowen Yu, Chengyuan
649 Li, Dayiheng Liu, Fei Huang, Haoran Wei, Huan Lin, Jian Yang, Jianhong Tu, Jianwei Zhang,
650 Jianxin Yang, Jiaxi Yang, Jingren Zhou, Junyang Lin, Kai Dang, Keming Lu, Keqin Bao, Kexin
651 Yang, Le Yu, Mei Li, Mingfeng Xue, Pei Zhang, Qin Zhu, Rui Men, Runji Lin, Tianhao Li, Tianyi
652 Tang, Tingyu Xia, Xingzhang Ren, Xuancheng Ren, Yang Fan, Yang Su, Yichang Zhang, Yu Wan,
653 Yuqiong Liu, Zeyu Cui, Zhenru Zhang, and Zihan Qiu. Qwen2.5 technical report, 2025. URL
654 <https://arxiv.org/abs/2412.15115>.

655 Jie Ren, Qipeng Guo, Hang Yan, Dongrui Liu, Quanshi Zhang, Xipeng Qiu, and Dahua Lin.
656 Identifying semantic induction heads to understand in-context learning, 2024. URL <https://arxiv.org/abs/2402.13055>.

657

658 Eric Todd, Millicent L. Li, Arnab Sen Sharma, Aaron Mueller, Byron C. Wallace, and David Bau.
659 Function Vectors in Large Language Models, February 2024.

660

661 Eduard Tulchinskii, Laida Kushnareva, Kristian Kuznetsov, Anastasia Voznyuk, Andrei Andriiainen,
662 Irina Piontkovskaya, Evgeny Burnaev, and Serguei Barannikov. Listening to the wise few: Select-
663 and-copy attention heads for multiple-choice qa, 2024. URL <https://arxiv.org/abs/2410.02343>.

664

665 Ashish Vaswani, Noam Shazeer, Niki Parmar, Jakob Uszkoreit, Llion Jones, Aidan N. Gomez, Lukasz
666 Kaiser, and Illia Polosukhin. Attention is all you need, 2023. URL <https://arxiv.org/abs/1706.03762>.

667

668 Kevin Wang, Alexandre Variengien, Arthur Conmy, Buck Shlegeris, and Jacob Steinhardt. Inter-
669 pretability in the wild: A circuit for indirect object identification in gpt-2 small, 2022. URL
670 <https://arxiv.org/abs/2211.00593>.

671

672 Sarah Wiegreffe, Oyvind Tafjord, Yonatan Belinkov, Hannaneh Hajishirzi, and Ashish Sabharwal.
673 Answer, assemble, ace: Understanding how lms answer multiple choice questions, 2025. URL
674 <https://arxiv.org/abs/2407.15018>.

675

676 Yukang Yang, Declan Campbell, Kaixuan Huang, Mengdi Wang, Jonathan Cohen, and Taylor Webb.
677 Emergent symbolic mechanisms support abstract reasoning in large language models, 2025. URL
678 <https://arxiv.org/abs/2502.20332>.

679

680 Kayo Yin and Jacob Steinhardt. Which attention heads matter for in-context learning?, 2025. URL
681 <https://arxiv.org/abs/2502.14010>.

682

683 Zifan Zheng, Yezhaohui Wang, Yuxin Huang, Shichao Song, Mingchuan Yang, Bo Tang, Feiyu
684 Xiong, and Zhiyu Li. Attention heads of large language models: A survey, 2024. URL <https://arxiv.org/abs/2409.03752>.

685

686

687

688

689

690

691

692

693

694

695

696

697

698

699

700

701

702 **A PROMPT EXAMPLES**
703
704 **A.1 OPEN-ENDED (5-SHOT)**
705
706 Q: resistant
707 A: susceptible
708
709 Q: classify
710 A: disorganize
711
712 Q: posterior
713 A: anterior
714
715 Q: goofy
716 A: serious
717
718 Q: stationary
719 A: moving
720
721 **A.2 MULTIPLE-CHOICE (3-SHOT)**
722
723 Instruction: Q: unveil A: ?
724 (a) optional
725 (b) mild
726 (c) con
727 (d) conceal
728 Response: (d)
729
730 Instruction: Q: hooked A: ?
731 (a) unhooked
732 (b) stale
733 (c) sturdy
734 (d) sell
735 Response: (a)
736
737 Instruction: Q: spherical A: ?
738 (a) unconstitutional
739 (b) flat
740 (c) demand
741 (d) healthy
742 Response: (b)
743
744 Instruction: Q: minute A: ?
745 (a) conservative
746 (b) hour
747 (c) retail
748 (d) awake
749 Response: (

750
751
752
753
754
755

B SIMILARITY MATRICES FOR OTHER MODELS

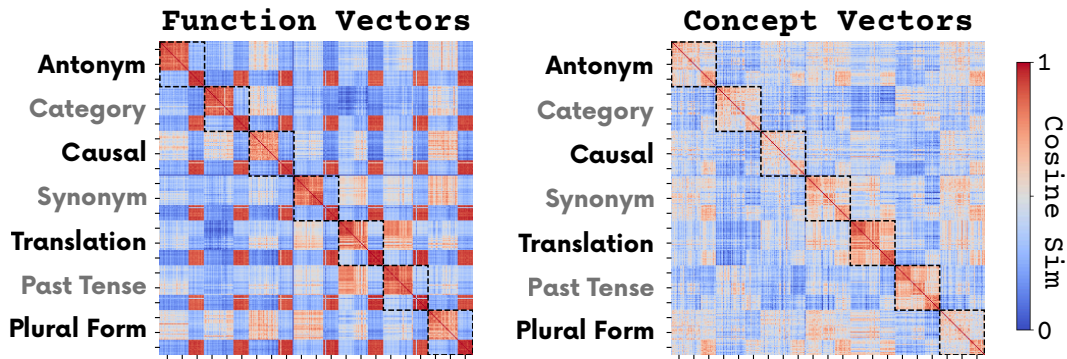


Figure 9: Similarity matrices extracted from top $K = 1$ heads in \mathcal{CV} s and \mathcal{FV} s in Llama 3.1 8B.

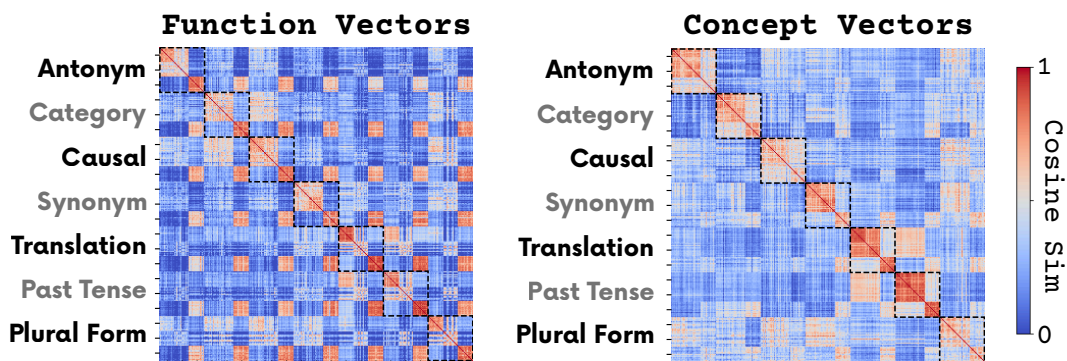


Figure 10: Similarity matrices extracted from top $K = 1$ heads in \mathcal{CV} s and \mathcal{FV} s in Qwen 2.5 7B.

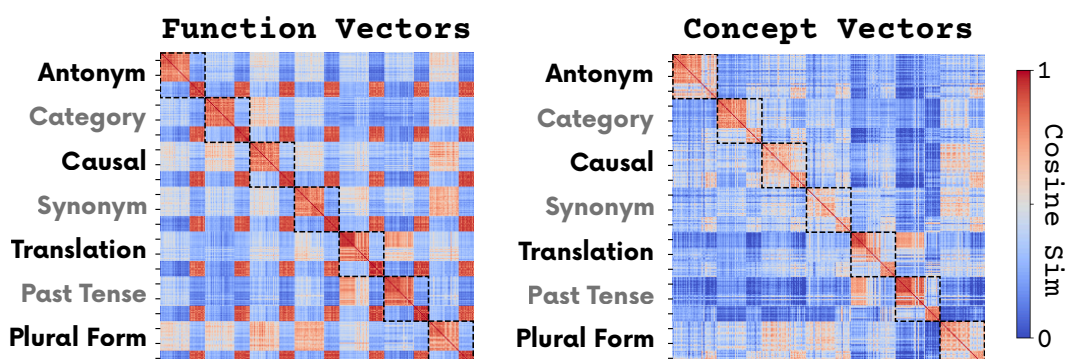


Figure 11: Similarity matrices extracted from top $K = 2$ heads in \mathcal{CV} s and \mathcal{FV} s in Owen 2.5 72B.

810
811

C AIE SCORES

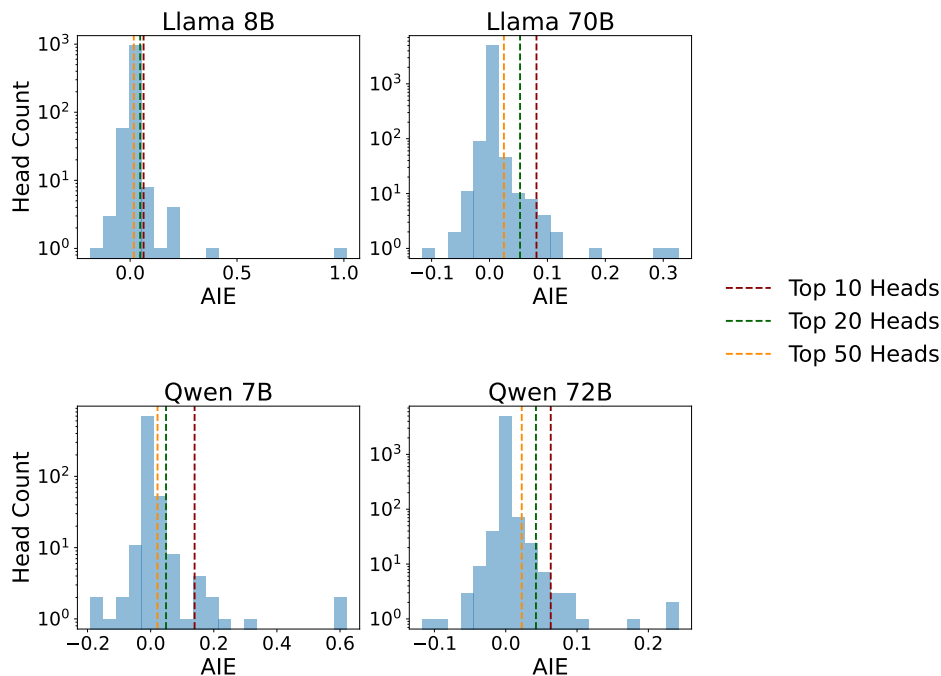
812
813
814
815
816
817
818
819
820
821
822
823
824

834
835

Figure 12: Histogram of AIE scores for Llama 3.1 8B, 70B, Qwen 2.5 7B, and Qwen 2.5 72B. Note,
836 the y-axis is on a log-scale. **Takeaway:** AIE scores are highly sparse.

837
838
839

D DATA GENERATION PROCESS

840
841
842
843

Concept sourcing: For most concepts (antonym, synonym, translation, present–past, singular–plural), we sourced word pairs from the datasets used by Todd et al. (2024). For categorical and causal concepts, we generated word pairs using OpenAI’s GPT-4o model (OpenAI, 2024).

844
845

Translation generation: French and Spanish translations were created using DeepL’s translation service (DeepL SE, 2025) to ensure high-quality, contextually appropriate translations.

846
847
848
849

Generated concepts (categorical and causal): We prompted GPT-4o to generate exemplar:category pairs (e.g., “apple:fruit”, “blue:colour”) and cause:effect pairs (e.g., “stumble:fall”, “storm:flood”). The model was given examples of the desired format and asked to produce 100 pairs per batch. We generated pairs in batches of 100 until reaching approximately 1000 examples per concept, with retry mechanisms to ensure sufficient coverage. The final datasets were saved as JSON files containing input-output pairs.

850
851
852

Quality filtering: Generated pairs underwent several filtering steps: (1) removal of duplicates based on input words, (2) exclusion of pairs containing underscores or numbers, (3) restriction to single words or two-word phrases (maximum one space per input/output), and (4) conversion to lowercase for consistency.

853
854
855

Multiple choice format: For multiple choice prompts, we generated four options per question by randomly sampling three additional outputs from the same concept dataset, ensuring all four options were unique. The correct answer was randomly positioned among the four options.

856
857
858
859
860
861
862
863

864 E SIGNIFICANCE TEST FOR RSA–AIE HEAD OVERLAP

865
 866 We assess whether the observed overlap between the top- K heads selected by Concept-RSA and by AIE is larger
 867 than expected by chance under a simple null model. Let N denote the total number of attention heads in the
 868 model (layers \times heads per layer). For a fixed K , each method selects a size- K subset of heads. Under the null
 869 hypothesis that these two subsets are independent, uniformly random size- K subsets of $\{1, \dots, N\}$, the overlap
 870 size

$$871 \quad X = |S_{\text{RSA},K} \cap S_{\text{AIE},K}|$$

872 follows a hypergeometric distribution $X \sim \text{Hypergeom}(N, K, K)$.

873 For an observed intersection x , we report the one-sided tail probability

$$874 \quad p_{\geq x} = \Pr[X \geq x] = \sum_{t=x}^K \frac{\binom{K}{t} \binom{N-K}{K-t}}{\binom{N}{K}}.$$

875 Entries with $p_{\geq x} < 0.05$ are typeset in bold in Table 1.

876 F STEERING HYPERPARAMETERS

877 To optimize the intervention performance, we conduct a hyperparameter search for two parameters:

- 878 • α : the steering weight that controls the strength of the intervention
- 879 • K : the number of attention heads to extract for concept vector computation

880 We evaluate the following parameter ranges:

- 881 • $K \in \{1, 3, 5, 10, 20, 50\}$ for the number of heads
- 882 • $\alpha \in \{1, 3, 5, 10, 15\}$ for the steering weight

883 The hyperparameter optimization is performed separately for each model using antonym prompts. We select the
 884 parameter combination that maximizes the average steering effect across all input formats. This ensures that our
 885 chosen hyperparameters generalize well across different prompt structures. We report the best hyperparameters
 886 for each model in Table 3.

887 Model	888 Best K	889 Best α
889 Llama 3.1 8B	1	10
890 Llama 3.1 70B	5	10
891 Qwen 2.5 7B	3	10
892 Qwen 2.5 72B	5	15

901 Table 3: Optimal hyperparameters for steering interventions across different models. K represents
 902 the number of attention heads used for $\mathcal{FV}/\mathcal{CV}$ extraction, while α controls the intervention strength.

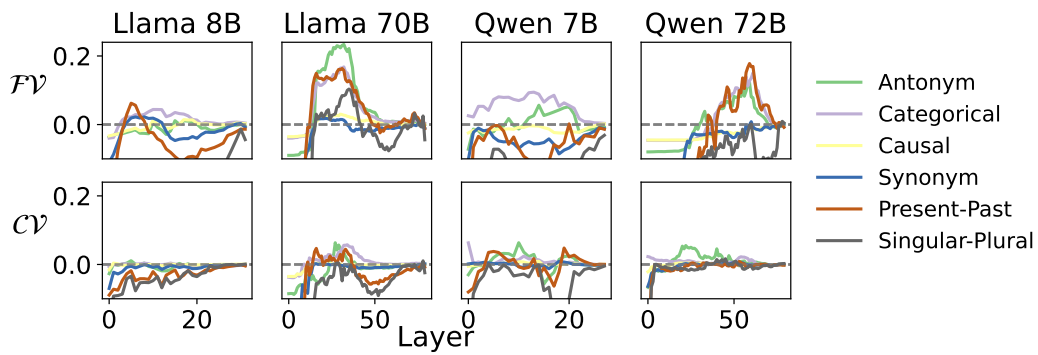
918 **G INPUT FORMAT MIXING IN FUNCTION VECTORS**
919
920

921
922
923
924
925
926
927
928
929
930
931
932
933
934
935
936
937
938
939
940
941
942
943
944
945
946
947
948
949
950
951
952
953
954
955
956
957
958
959
960
961
962
963
964
965
966
967
968
969
970
971

Figure 13: ΔP for French translations of all the concepts. $\mathcal{F}\mathcal{V}$ s and $\mathcal{C}\mathcal{V}$ s are extracted from open-ended French prompts.

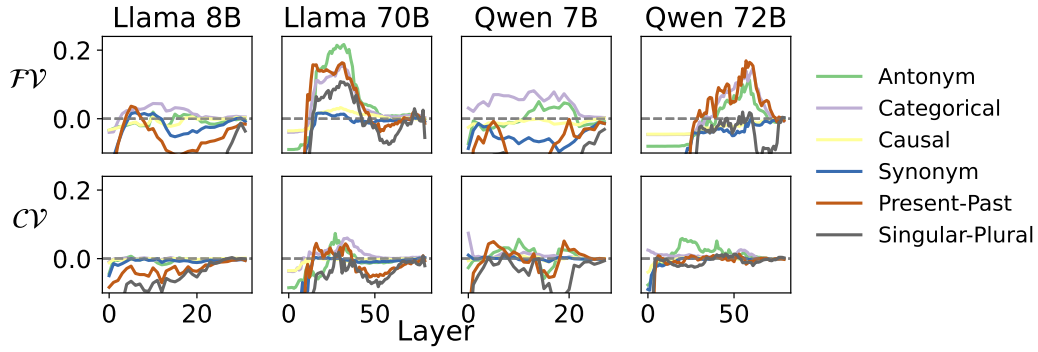

950
951
952
953
954
955
956
957
958
959
960
961
962
963
964
965
966
967
968
969
970
971

Figure 14: ΔP for French translations of all the concepts. $\mathcal{F}\mathcal{V}$ s and $\mathcal{C}\mathcal{V}$ s are extracted from open-ended Spanish prompts.

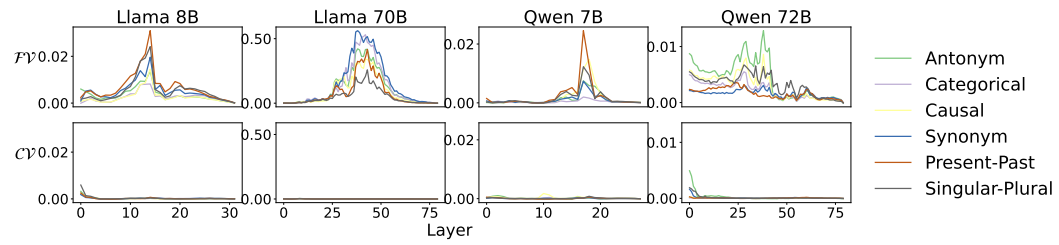
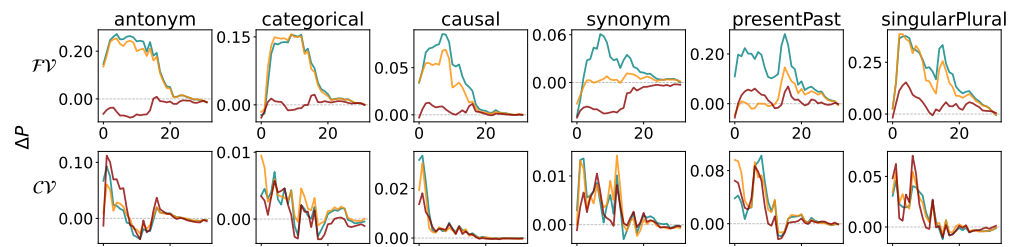
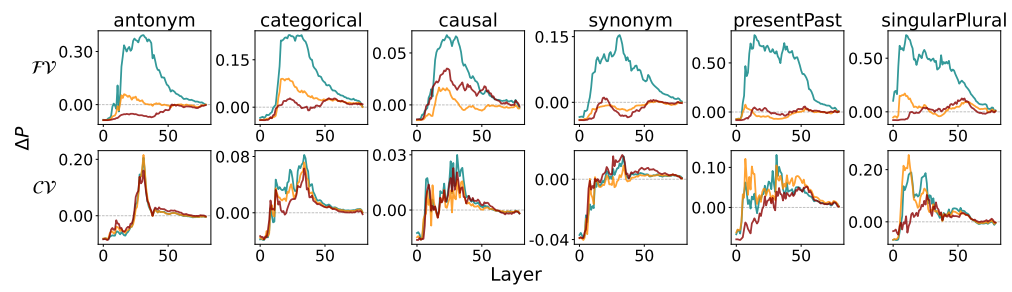

960
961
962
963
964
965
966
967
968
969
970
971

Figure 15: ΔP for the opening bracket token `_`. $\mathcal{F}\mathcal{V}$ s and $\mathcal{C}\mathcal{V}$ s are extracted from multiple-choice prompts.

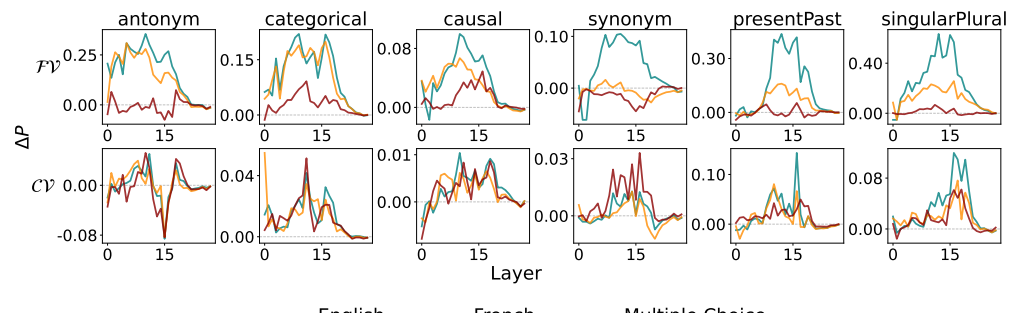
972 H STEERING RESULTS



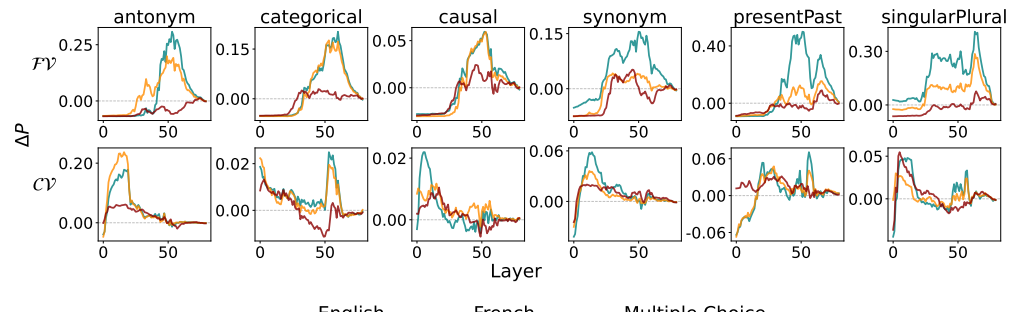
986 (a) Llama 3.1 8B



996 (b) Llama 3.1 70B



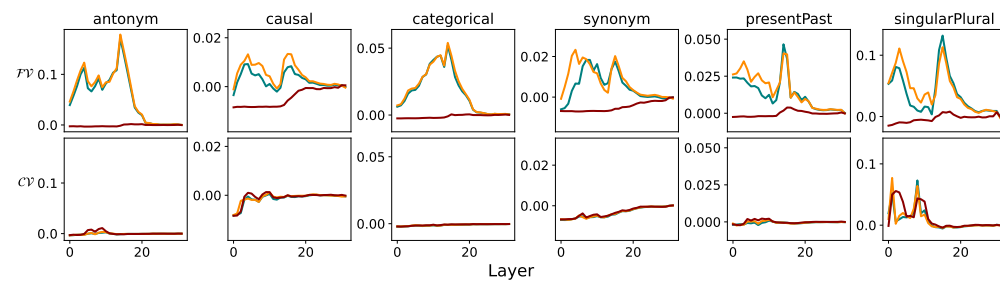
1011 (c) Qwen 2.5 7B



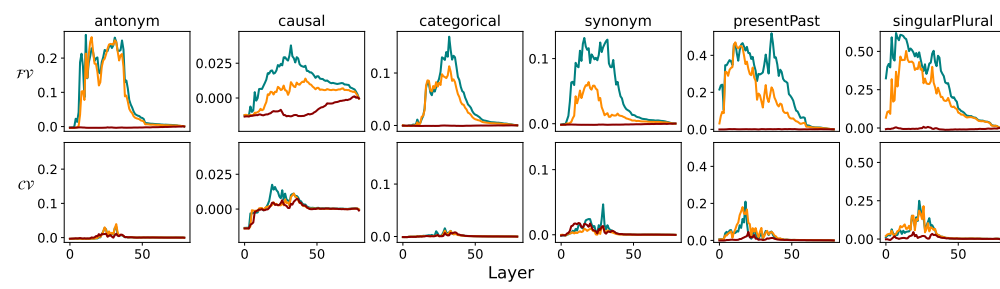
1024 (d) Qwen 2.5 72B

1025 Figure 16: Steering effect across layers and all concepts for different models.

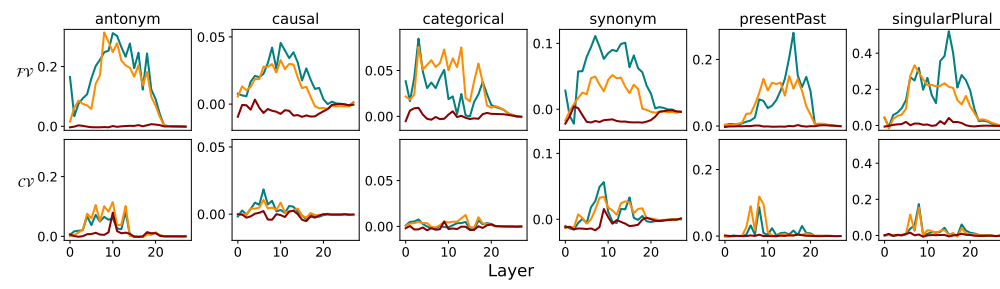
1026 I 0-SHOT STEERING RESULTS
1027
1028



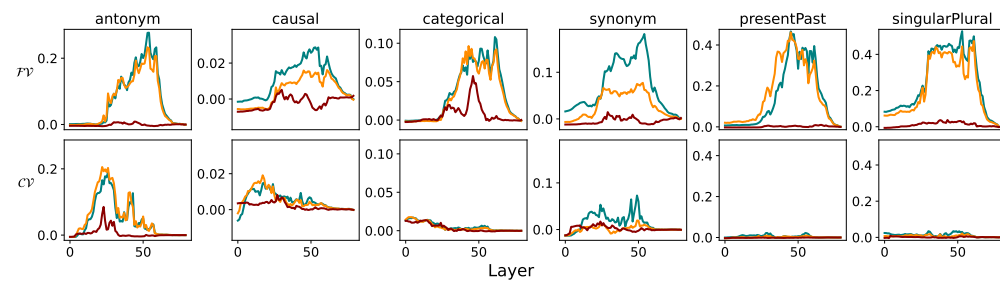
(a) Llama 3.1 8B



(b) Llama 3.1 70B



(c) Qwen 2.5 7B

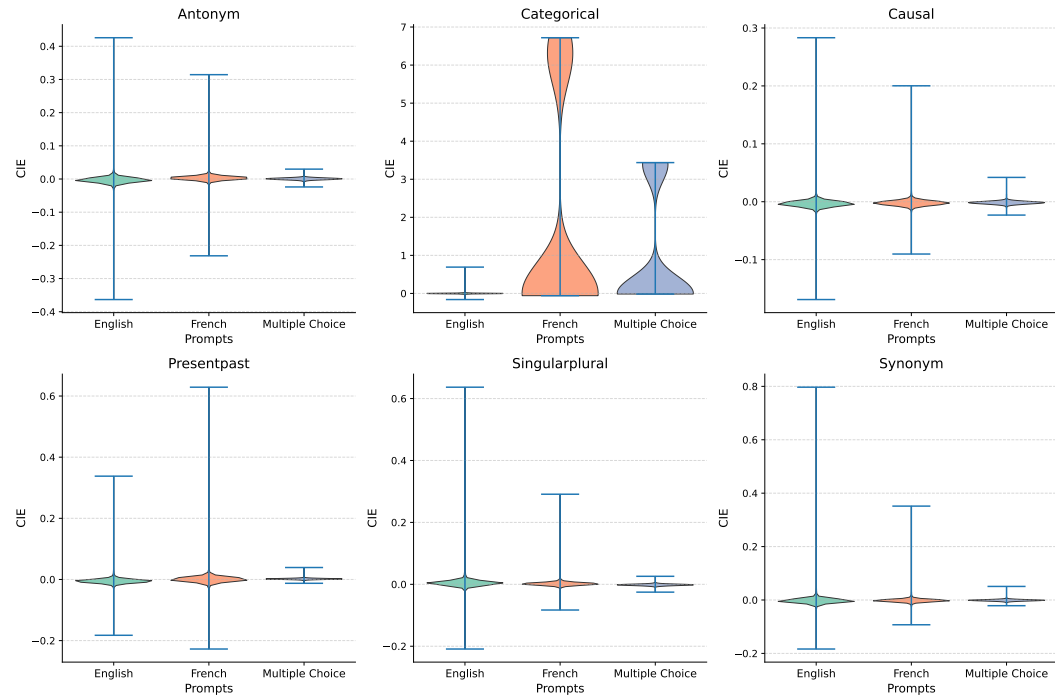


(d) Qwen 2.5 72B

Figure 17: 0-shot steering effect across layers and all concepts for different models.

1080 J QWEN 2.5 72B OUTLIER ANALYSIS

1081
 1082 We identified anomalous CIE values for Qwen 2.5 72B in the Categorical concept across French open-ended
 1083 and multiple-choice formats. As shown in Figure 18, these conditions exhibit unusually high CIE values with a
 1084 bimodal distribution that deviates from the expected pattern. We excluded these two datasets from the final AIE
 1085 calculations. This exclusion has minimal impact on our results: the top-5 head rankings remain identical (100%
 1086 overlap), confirming that our main findings are robust to this methodological decision.



1109 Figure 18: Violin plots of CIE for different concepts and prompts.

1110
 1111
 1112
 1113
 1114
 1115
 1116
 1117
 1118
 1119
 1120
 1121
 1122
 1123
 1124
 1125
 1126
 1127
 1128
 1129
 1130
 1131
 1132
 1133

1134
1135 **K DISENTANGLING FORMAT-SPECIFIC AND ABSTRACT REPRESENTATIONS IN**
1136 **FUNCTION VECTORS**

1137 Multiple-choice (MC) format involves distinct computational steps beyond open-ended generation: evaluating
1138 options, comparing candidates, and selecting among labeled alternatives (Tulchinskii et al., 2024; Wiegreffe
1139 et al., 2025). When FV heads are extracted from MC prompts, they must therefore capture both (a) the
1140 task representation (e.g., antonym, causation) and (b) the MC-specific formatting demands. We test whether
1141 partitioning out of the MC information, makes the task representation abstract, i.e., is shared across all formats?

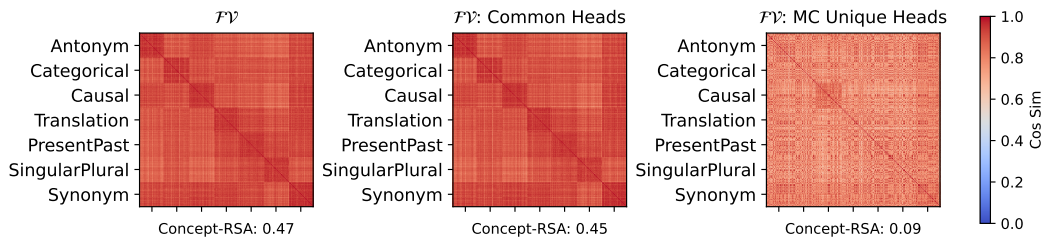
1142 We partition FV heads in Llama 3.1 70B into three subsets:

- 1144 • **All Heads:** Top-5 heads identified by AIE computed over all input formats (standard FV selection, Eq.
1145 5)
- 1146 • **Common Heads:** Heads that appear in the top-10 heads for *all three* input formats independently. (3
1147 heads).
- 1148 • **Unique MC Heads:** Heads that appear in the top-10 heads for MC format only. (6 heads)

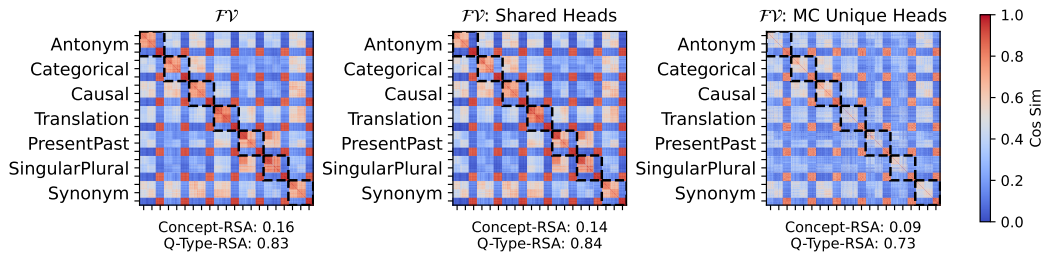
1149 If abstract task representations exist in FVs independent of format, we would expect them to reside primarily in
1150 the **common heads** that are causally important across all formats. We then computed similarity matrices and
1151 RSA scores for each head subset.

1152 We see that within the MC format, common heads cluster by concept (Figure 19), but the representations are
1153 nearly orthogonal between open-ended and multiple-choice prompts for the same concept (Figure 20).

1154 It is still possible that these heads could encode both abstract task in open-ended and format features in MC
1155 prompts in superposition. However, under the Linear Representation Hypothesis (Park et al., 2024), a shared
1156 abstract concept should occupy a consistent linear subspace detectable via cosine similarity. The observed
1157 orthogonality across formats implies that any abstract representation is not linearly accessible in a format-
1158 invariant way. This suggests that FVs encode tasks at a lower level of abstraction (i.e., ‘antonym in MC format’)
1159 rather than a shared, format-independent concept.



1169 **Figure 19: Similarity matrices for MC prompts only.** Each panel shows the similarity matrix
1170 for a different subset of AIE-selected heads computed over MC prompts only (7 concepts \times 50
1171 prompts each). Common heads show stronger concept clustering than unique MC heads (albeit with
1172 large similarity between concepts due to the shared MC structure). Full FVs show a very similar
1173 representational structure to the common heads. Model: Llama 3.1 70B.



1184 **Figure 20: Similarity matrices for different FV head subsets across all formats.** Same as Figure 19 but
1185 computed over all input formats (7 concepts \times 3 formats \times 50 prompts). Within the same concept
1186 the representations are nearly orthogonal between open-ended and multiple-choice prompts. Model:
1187 Llama 3.1 70B.

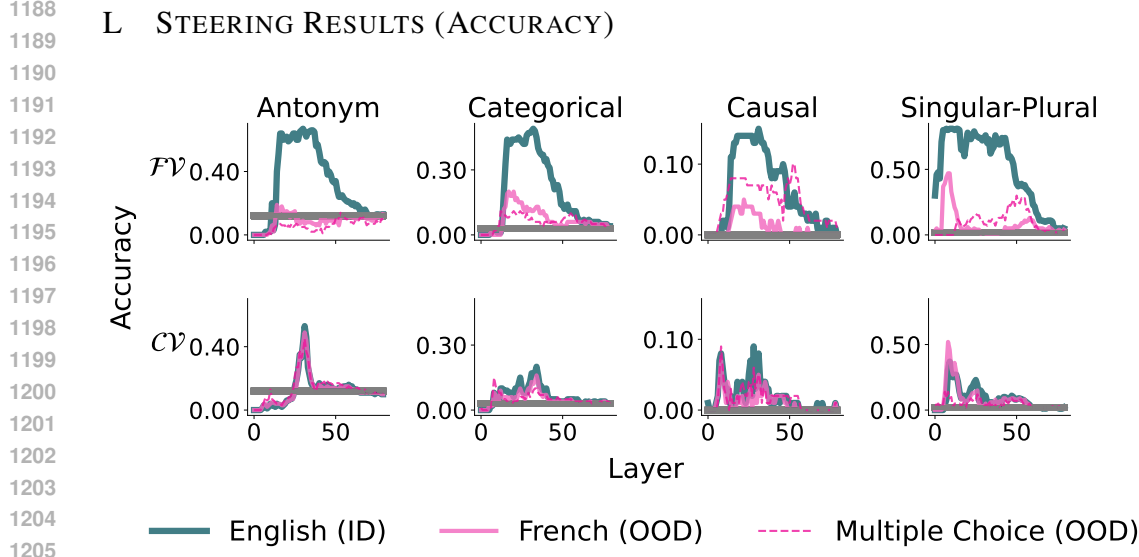


Figure 21: *Steering effect across layers (Accuracy)*. We inject \mathcal{CV} s and $\mathcal{F}\mathcal{V}$ s into Llama-3.1-70B and plot the Top-1 accuracy for four representative concepts (columns). The grey horizontal line indicates the accuracy of the unsteered model. See Figure 7 for ΔP results.

M MULTIPLE-CHOICE FORMAT WITH WORDS AS OUTPUT

Example prompt:

```
1215 Instruction: Q: spherical A: ?
1216 unconstitutional
1217 flat
1218 demand
1219 healthy
1220 Response: flat
1221 Instruction: Q: unveil A: ?
1222 optional
1223 mild
1224 sturdy
1225 conceal
1226 Response:
```

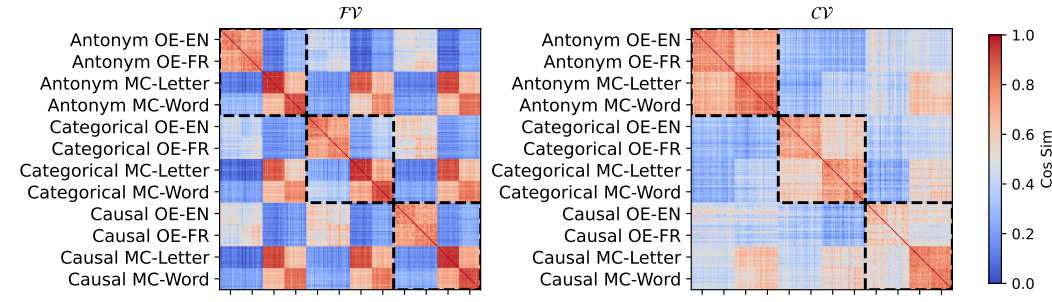


Figure 22: Similarity matrices for $\mathcal{F}\mathcal{V}$ s and \mathcal{CV} s with the inclusion of MC prompts where the model is expected to produce a word instead of a letter. **Takeaway:** Unlike \mathcal{CV} s, $\mathcal{F}\mathcal{V}$ MC representations still cluster due to the input format, therefore MC cluster effect is not due to the model producing words/letters. Model: Llama 3.1 70B.

1242 N AMBIGUOUSICL IN DIFFERENT LANGUAGES

1243

1244

1245 In the original AmbiguousICL implementation, the concepts are presented in English and the translations are
1246 presented in French.

1247 Here, we test the effect of presenting the concepts in a different language to determine if \mathcal{CV} s are tied to a
1248 specific surface form (e.g., “English Antonym”). Specifically, we present the concepts in Spanish and interleave
1249 them with Spanish-to-English translations.

1250 Example antonym prompt:

1251

1252 Q: final
1253 A: inicial

1254

1255 Q: inmaduro
1256 A: madura

1257

1258 Q: norte
A: sur

1259

1260 Q: descendiente
A: descendant

1261

1262 Q: probablemente
A: probable

1263

1264 Q: vivo
A:

1265

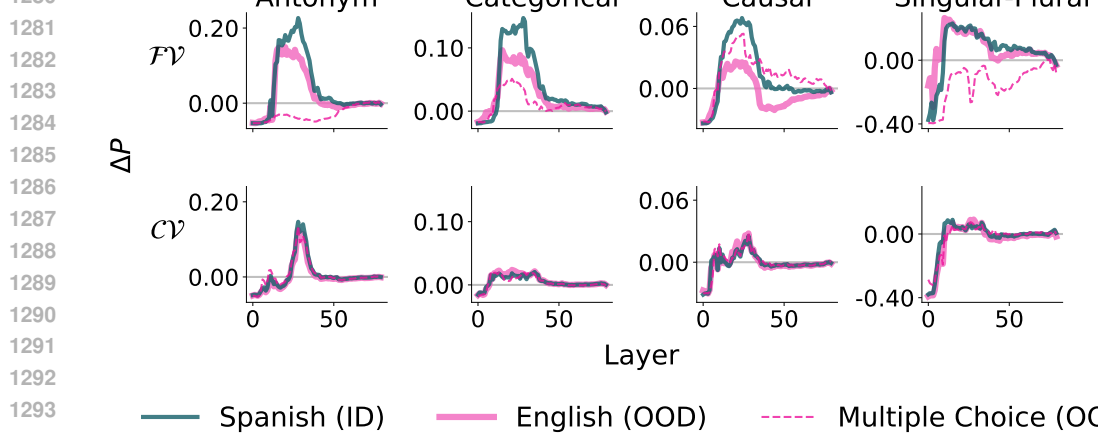
1266 The expected response is the Spanish antonym ‘vivo’ → ‘muerto’. Therefore, the ID vectors are extracted
1267 from open-ended Spanish antonym prompts and the OOD vectors are extracted from open-ended English and
1268 multiple-choice prompts.

1269 In Figure 23, we see that the steering effect trends are similar to the original implementation (although the
1270 absolute performance is lower for both \mathcal{CV} s and \mathcal{FV} s). In Figure 24, we also see that the KL divergence is
1271 lower for the \mathcal{CV} s compared to the \mathcal{FV} s. Crucially, the \mathcal{CV} s (extracted from English) steer the model to produce
1272 the **Spanish antonym** (the contextually appropriate response), rather than the English antonym or the English
1273 translation. This demonstrates that \mathcal{CV} s encode the abstract ‘Antonym’ concept rather than ‘English Antonym’.
1274 Mechanistically, this suggests that the \mathcal{CV} amplifies the task probability (“do an antonym”) while relying on the
1275 prompt’s existing context to determine the surface form (“in Spanish”), rather than injecting language-specific
1276 content.

1277

1278

1279



1293 Figure 23: Steering effect across layers and all concepts for different languages.
1294
1295

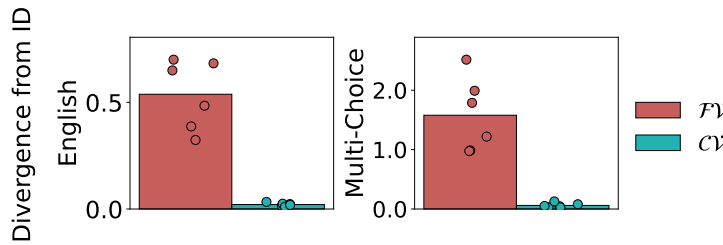


Figure 24: KL divergence between ID and OOD for different languages. Model: Llama 3.1 70B.

O CROSS-FORMAT ACTIVATION PATCHING

To determine whether the dissociation between causal (FV) and invariant (CV) heads stems from the activation patching setup—specifically, whether patching within the same format biases results toward format-specific heads—we conducted cross-format activation patching across all 6 combinations of input formats. In this experiment, we extracted activations from clean prompts in one format (e.g., Open-Ended English) and patched them into a corrupted run of a different format (e.g., Multiple-Choice).

We found that cross-format patching consistently identified a subset of the original Function Vector heads (e.g., in Llama-3.1-70B, head L31H18 always appears in the top-5 for both within-format and cross-format patching). It did not identify Concept Vector heads. This result shows that FVs are the primary causal mechanism for the task across all formats, despite their representations being format-specific. CVs, while representationally invariant, do not appear to causally drive the model’s behavior in these tasks.

Source Format	Target Format	Max AIE	Overlap w/ FV (top-5)	Overlap w/ CV (top-5)
OE-ENG	OE-FR	0.22	4	0
OE-ENG	MC	0.02	2	0
OE-FR	MC	0.01	1	0
MC	OE-ENG	0.23	3	0
OE-FR	OE-ENG	0.41	4	0
MC	OE-FR	0.12	4	0

Table 4: *Cross-format Activation Patching Results (Llama 3.1 70B)*. We show the max Average Indirect Effect (AIE) and the number of overlapping heads with the standard Function Vectors (FV) and Concept Vectors (CV) (top-5 heads). The patching source refers to the format from which activations were extracted, and the target refers to the corrupted prompt format into which they were patched. FV heads are consistently identified across formats (specifically L31H18 and L35H57), while CV heads are not.